Response to the review of the manuscript: "The Dissipation of Shallow Cumulus Clouds: Dynamics, Microphysics, and Environmental Signatures"

We would like to thank the editor and the two reviewers for their efforts and beneficial comments, which helped us improve and clarify the manuscript. We have addressed all the comments in a point by point manner and revised the manuscript accordingly.

Before presenting our specific answers to all the reviewers' comments and questions, we open with a short summary of the main changes made in the revised manuscript:

- **Expanded the model and simulation description** to improve reproducibility, including the SAM configuration, BOMEX case study initialization and forcing, boundary conditions, turbulence parameterization, radiation treatment, and aerosol activation and regeneration processes.
- **Clarified the distinction between cloud droplets and raindrops** in the spectral-bin microphysics scheme and the definition of total liquid water content used for cloud identification and analysis. Additional supplementary figures present cloud-droplet-only analysis to distinguish cloud-droplet evolution from the contribution of precipitation-sized drops.
- **Expanded the CCN sensitivity analysis** in the Results and Conclusions, highlighting similarities and differences in cloud evolution across CCN concentrations and strengthening comparisons with previous studies.
- **Expanded the discussion of the study's limitations**, particularly the use of isolated clouds and hence the absence of cloud–cloud interactions, the simplified background wind conditions, and the exclusion of interactive cloud-dependent radiative effects.

Please see below the specific answers to all the comments (marked in blue).

Reviewer #1:

General assessment

This manuscript investigates the dissipation stage of isolated shallow trade cumulus clouds using high-resolution simulations with spectral-bin microphysics and varying CCN concentrations. The authors analyze the evolution of cloud dynamics, turbulence, microphysics, and the near-cloud environment during cloud decay, and document features such as the emergence of a humid halo, enhanced near-cloud vorticity, and changing turbulent versus coherent kinetic energy contributions. The topic is scientifically interesting, and the manuscript is generally well written. The dissipation stage of shallow cumulus clouds has received considerably less attention than the growth and mature stages, and this study contributes useful process-level insights into the structure and evolution of dissipating clouds.

I believe this manuscript has the potential to make a valuable contribution to ACP. However, I also believe that substantial revisions are necessary before publication. My primary concerns relate to (1) the articulation of the scientific advances associated with the CCN sensitivity experiments, (2) ambiguity regarding the treatment and interpretation of cloud versus precipitation hydrometeors

throughout the analysis, and (3) insufficient methodological detail to ensure reproducibility. I therefore recommend major revisions.

Answer: We are glad the reviewer found the work scientifically interesting and the manuscript well written. We answered the three mentioned points and changed the manuscript accordingly. Please see the full details below.

Major comments

1. The conclusions regarding CCN sensitivity are not sufficiently developed.

My main concern is that the conclusions primarily focus on the overall evolution of the simulations rather than on specific conclusions arising from the sensitivity to CCN concentration. Indeed, the final paragraph of the conclusions contains almost no discussion of CCN sensitivity, despite the manuscript being built around five simulations spanning a wide range of aerosol concentrations.

The primary conclusion from the sensitivity study is summarized as: "The microphysical evolution during dissipation depends strongly on aerosol loading and precipitation formation." This statement is broadly expected from previous literature. The manuscript would benefit from a clearer articulation of what is genuinely new and quantitatively distinct about the present results.

For example, I find it noteworthy that the cloud macrophysical evolution (Figure 2) and the TKE/CKE evolution (Figure 4) of the polluted, non-precipitating clouds appear remarkably insensitive to CCN concentration. That result seems potentially important, yet it is not highlighted or discussed in depth.

Similarly, several conclusions related to the evolution of effective radius, DSD width, humid halos, enhanced turbulence, and evolving near-cloud circulations appear qualitatively consistent with prior studies cited in the introduction. The manuscript would be strengthened by explicitly discussing how the findings agree with, differ from, or extend studies such as Lim and Hoffmann (2024) and Zhang et al. (2011). The unique findings emerging from the CCN sensitivity experiments should be stated more clearly and quantified wherever possible.

More generally, I found myself asking throughout the conclusions: what have we learned specifically because five CCN concentrations were simulated?

Answer: We thank the reviewer for this important comment. We have therefore expanded the Results and Conclusions to provide a clearer comparison across CCN concentrations, highlighting both the similarities and differences in cloud evolution.

The five simulations reveal that the response to CCN concentration differs among cloud properties and is strongly associated with whether precipitation develops. The most pronounced differences occur between the precipitating and non-precipitating clouds. In particular, the precipitating cases exhibit larger and later peaks in total liquid water mass and cloud volume, as well as differences in the temporal evolution of TKE and CKE.

An important finding is that the three non-precipitating clouds exhibit remarkably similar total liquid water mass and energetic evolution, despite the substantial range of initial CCN concentrations. However, their macrophysical properties are not entirely insensitive to CCN concentration: mean LWC increases and cloud volume generally decreases with increasing CCN concentration. These results indicate that cloud geometry and liquid water distribution may change even when the evolution of total liquid water mass remains similar.

The near-cloud properties also exhibit different responses to aerosol loading. The magnitude of the near-cloud enstrophy anomaly increases with CCN concentration, whereas the humid-halo anomaly does not show a clear monotonic dependence.

We have revised the Results and Conclusions to emphasize these findings and to better distinguish the effects of CCN concentration on the different aspects of cloud dissipation. We have also expanded the discussion of the microphysical results to clarify their agreement with and differences from previous studies, particularly Zhang et al. (2011) and Lim and Hoffmann (2024).

The revised Results section 3.1.1:
"Notably, despite their different initial CCN concentrations, the three non-precipitating cases exhibit similar total liquid water mass evolution, with comparable peak values and subsequent declines (Fig. 2b). Nevertheless, within these cases, increasing CCN concentration is generally associated with higher mean LWC and smaller cloud volumes (Fig 2a,e), indicating that similar total liquid water mass does not necessarily imply similar cloud structure. This behavior is consistent with previous LES studies of shallow trade cumulus clouds, which showed that increasing aerosol concentrations produce smaller droplets that evaporate more readily during entrainment, thereby enhancing evaporation near cloud boundaries and reducing cloud size (Xue et al. 2006, Seigel et al. 2014)."

Section 3.1.3:
"Notably, despite their different initial CCN concentrations, the three non-precipitating cases exhibit similar temporal evolution of both TKE and CKE, with comparable peak magnitudes and subsequent declines (Fig. 4a)."

The revised Conclusions now include the following passages:

"The microphysical evolution during dissipation depends strongly on aerosol loading and precipitation formation. In the precipitating cases, droplet number concentration decreases markedly near cloud top once the clouds reach the inversion, due to collision-coalescence, and this reduction progressively propagates downward through the cloud during dissipation. At the same time, effective radius and DSD width increase strongly, consistent with the formation of a relatively small number of large raindrops. In the more polluted, non-precipitating cases, these signatures are weaker: although droplet concentrations gradually decrease over time, they remain relatively high aloft throughout most of the cloud lifetime, while effective radius and DSD width profiles change only modestly with time, making them poor indicators of the cloud life cycle stage. These findings are broadly consistent with Zhang et al. (2011), who reported a modest decrease in effective radius during dissipation in polluted and moderately polluted clouds, whereas clean clouds exhibited larger effective radii and greater variability associated with collision-coalescence and sedimentation. Similarly, our results show greater changes in effective radius in the precipitating low-CCN cases, while the non-precipitating cases exhibit relatively weak temporal variability. Notably, the microphysical properties in the non-precipitating clouds exhibit weaker temporal than vertical variability, indicating that changes in the DSD are more strongly associated with vertical structure than with cloud age alone. This behavior is also consistent with a microphysical response to mixing that occurs on a shorter timescale than the mixing process itself: as dry environmental air is progressively entrained, exposed droplets can evaporate rapidly, reducing droplet number concentration while leaving the mean size of the remaining droplet population relatively unchanged. This interpretation is consistent with Lim and Hoffmann (2024), who showed that inhomogeneous mixing becomes increasingly important over the cloud life cycle. This is also consistent with the

ergodicity framework of Lensky and Rosenfeld (2006), who showed from satellite observations of convective clouds that droplet effective radius depends primarily on height and thermodynamic conditions, while exhibiting relatively weak temporal variability over the cloud lifetime. Similar behavior was reported in the in situ observations of Schmeissner et al. (2015), who found that dissipating clouds exhibit reduced liquid water content and droplet number concentration, whereas droplet sizes remain nearly unchanged relative to developing clouds."

"The five CCN sensitivity experiments reveal that the influence of aerosol loading during dissipation differs among cloud properties. The largest differences are observed between the precipitating and non-precipitating clouds. In particular, the precipitating cases exhibit larger and later peaks in total liquid water mass and cloud volume, together with differences in the temporal evolution of TKE and CKE. In contrast, the three non-precipitating simulations show remarkably similar total liquid water mass and energetic evolution, despite their substantial differences in initial CCN concentration. Nevertheless, increasing CCN concentration within the non-precipitating regime is associated with higher mean LWC and generally smaller cloud volumes, indicating that cloud structure remains sensitive to aerosol loading even when the total liquid water mass evolves similarly. This may reflect enhanced evaporation of smaller droplets and stronger turbulent erosion near cloud boundaries at higher CCN concentrations. The near-cloud signatures also exhibit different responses: the magnitude of the enstrophy anomaly increases with CCN concentration, whereas the humid-halo anomaly does not exhibit a clear monotonic dependence. Together, these findings demonstrate that the sensitivity of cloud dissipation to CCN concentration is not uniform across cloud properties."

2. The distinction between cloud droplets and rain drops is unclear and affects interpretation of many results.

A second major concern is the lack of a clear distinction between cloud droplets and precipitation-sized particles throughout the manuscript.

The manuscript never explicitly states how cloud droplets and raindrops are separated within the spectral-bin scheme. For example, are bins 1-16 considered cloud droplets and bins 17-33 considered rain drops (or some similar convention)? If so, this should be explicitly stated.

This ambiguity creates difficulties when interpreting multiple figures and conclusions. For example, at line 146, LWC is defined as cloud liquid water content. My initial interpretation was the conventional one: liquid water associated with cloud droplets only. As I continued reading, however, I became uncertain whether LWC instead represents the sum across all 33 hydrometeor bins, including precipitation.

I therefore found it difficult to determine whether many of the reported signatures reflect modifications to the cloud droplet population or simply the emergence of rain water.

I believe the analysis would be substantially clearer if the conventional cloud-water definition were employed throughout the manuscript. In particular, Figure 1 would be more informative if cloud liquid water (cloud droplets: bins 1-16) and precipitation water (bins 17-33) were presented separately. Several other analyses may also benefit from separating cloud and precipitation contributions.

Answer: We thank the reviewer for this important comment. In our spectral-bin microphysics scheme, cloud droplets are represented by bins 1–15, with bin 15 corresponding to a droplet size of

50.8 μm, whereas bins 16–33 represent precipitation-sized drops. We have revised the Methods section to explicitly state this distinction and clarify the definition of liquid water content used in the different analyses.

In the original analysis, LWC was calculated as the sum of cloud-droplet water and rainwater, including all 33 bins, above cloud base height (600 m). This definition was also used for cloud identification and tracking, with a threshold of 0.01 g kg^{-1}. We now explicitly distinguish between cloud-droplet water, rainwater, and their sum to avoid confusion when interpreting the results.

To further assess the contribution of precipitation-sized drops to the reported cloud properties, we have added supplementary analyses that consider only the cloud-droplet population (bins 1–15). Supplementary Figure S2 presents the vertical cross-sections of the cloud droplet water content field [g kg^{-1}]. Figure S3 presents the corresponding bulk cloud properties calculated using only the cloud droplets, allowing comparison with the original analysis that includes both cloud droplets and raindrops. Similarly, Supplementary Figure S6 presents the Hovmöller diagrams of droplet number concentration, effective radius, and DSD width calculated using only bins 1–15. These additional analyses allow the cloud-droplet evolution to be examined separately from the influence of precipitation-sized drops.

We have also revised the relevant figure descriptions and captions to explicitly indicate whether the quantities are calculated using all hydrometeor bins or only the cloud-droplet population. These revisions clarify the interpretation of the microphysical and bulk cloud properties and allow the effects of precipitation formation to be distinguished more clearly from changes in the cloud-droplet population.

The revised method:

"A cloud identification procedure was used to isolate the main cloud generated by the initial thermal perturbation, excluding secondary clouds from the analysis. In the spectral-bin microphysics scheme, cloud droplets are represented by bins 1-15, with bin 15 corresponding to a droplet radius of 50.8 μm, whereas bins 16-33 represent raindrops. Cloud objects were identified using the total liquid water mixing ratio, defined as the sum of cloud-droplet water and rainwater (all 33 bins), with a threshold of $LWC = 0.01 \frac{g}{kg}$"

Revised results:

Section 3.1.1:

"Cross-sections of the cloud total liquid water content (LWC) at selected times are shown in Fig.1 . During the developing stage, all clouds show increasing LWC with height, with the largest values near the cloud top. As the clouds evolve, clear differences emerge between the clean and polluted cases: in the clean simulations, dissipation is strongly influenced by precipitation, whereas in the polluted simulations, the clouds do not precipitate and decay mainly through evaporation and mixing. The figure also suggests narrowing of the cloudy region during dissipation, especially in the polluted cases; the responsible processes are examined in more detail below. The corresponding cross-sections considering only cloud droplets (bins 1-15) are shown in Supplementary Figure S2, allowing the contribution of precipitation-sized drops to be distinguished. Figure S2 also highlights differences between the precipitating and non-precipitating clouds. At the beginning of dissipation, cloud droplets occupy a larger area of the cloud cross-section in the precipitating cases than in the non-

precipitating cases. However, this area decreases substantially as dissipation progresses, leaving only a small region containing cloud droplets during advanced dissipation."

"Figure 2 presents the clouds' evolution through time series of several bulk properties for all simulated cases. They are calculated for the cloudy voxels of the main cloud only, defined by a total liquid water mixing ratio (cloud droplets and raindrops) greater than 0.01 $\frac{g}{kg}$ *and located above 600 m (cloud base). Figure S3 presents the corresponding analysis considering only cloud droplets (bins 1-15), allowing examination of the influence of precipitation-sized drops on the bulk cloud properties. These bulk properties provide an integrated description of the cloud state and can therefore be useful for identifying the signature of the different stages along the cloud's life cycle. The peaks in cloud-mean LWC (Fig. 2a) and cloud-top height (Fig. 2d), together with the first transition of the mean buoyancy from positive to negative (Fig. 2c), occur within a relatively narrow time window, between 32–35 min, across all simulations. By contrast, the maxima in cloud volume (Fig. 2e) and cloud area (Fig. 2f) occur later, after 35 min, and show larger differences among the cases. For cloud volume, cloud area, and cloud-total liquid mass (Fig. 2b), the precipitating cases peak a few minutes later than the non-precipitating cases, reflecting the onset of rain formation and the spread of falling hydrometeors along the cloud sides, which increase the apparent cloud extent and volume. Notably, despite their different initial CCN concentrations, the three non-precipitating cases exhibit similar total liquid water mass evolution, with comparable peak values and subsequent declines (Fig2 b). Nevertheless, within these cases, increasing CCN concentration is generally associated with higher mean LWC and smaller cloud volumes (Fig 2a,e), indicating that similar total liquid water mass does not necessarily imply similar cloud structure . In the cloud-droplet-only analysis (Fig. S3), the precipitating cases exhibit lower liquid water mass and smaller cloud volume and horizontal area compared with the corresponding total-liquid-water analysis (Fig. 2). In addition, when only cloud droplets are considered, the peaks in liquid water mass and cloud volume occur a few minutes earlier and approximately coincide with those in the non-precipitating cases. A comparison of Figs. 1 and S2 shows that raindrops fall along the cloud edges, extending the region containing liquid water beyond the cloud-droplet region. These differences further indicate that precipitation-sized drops contribute to the later peaks in liquid water mass and cloud volume, as well as to the larger apparent cloud extent observed in the total-liquid-water cross-sections."*

Section 3.2.1:

"The corresponding Hovmöller diagrams considering only cloud droplets (bins 1-15) are shown in Supplementary Figure S6. They exhibit broadly similar temporal and vertical patterns to those obtained using all hydrometeor bins (Fig.5), but with smaller effective radii and DSD standard deviations."

The revised caption of figure 5: "*Hovmöller diagrams of horizontally averaged cloud microphysical properties plotted on a logarithmic color scale calculated using all 33 hydrometeor bins (cloud droplets and raindrops). The top row shows droplet number concentration [*cm^{-3}*], the middle row shows effective radius [*μm*], and the bottom row shows standard deviation of the drop size distribution (DSD) [*μm*]. Columns correspond to simulations initialized with different CCN concentrations (left to right): 25, 50, 250, 500, and 2000* cm^{-3}*. Within each row, the two leftmost panels (precipitating cases) and the three rightmost panels (non-precipitating cases) use separate color scales to better visualize their respective value ranges. The corresponding Hovmöller diagrams plotted using linear color scales are shown in Supplementary Figure S5. Supplementary Figure S6*

presents the corresponding analysis considering only cloud droplets (bins 1-15), allowing the evolution of the cloud-droplet population to be examined separately from precipitation-sized drops"

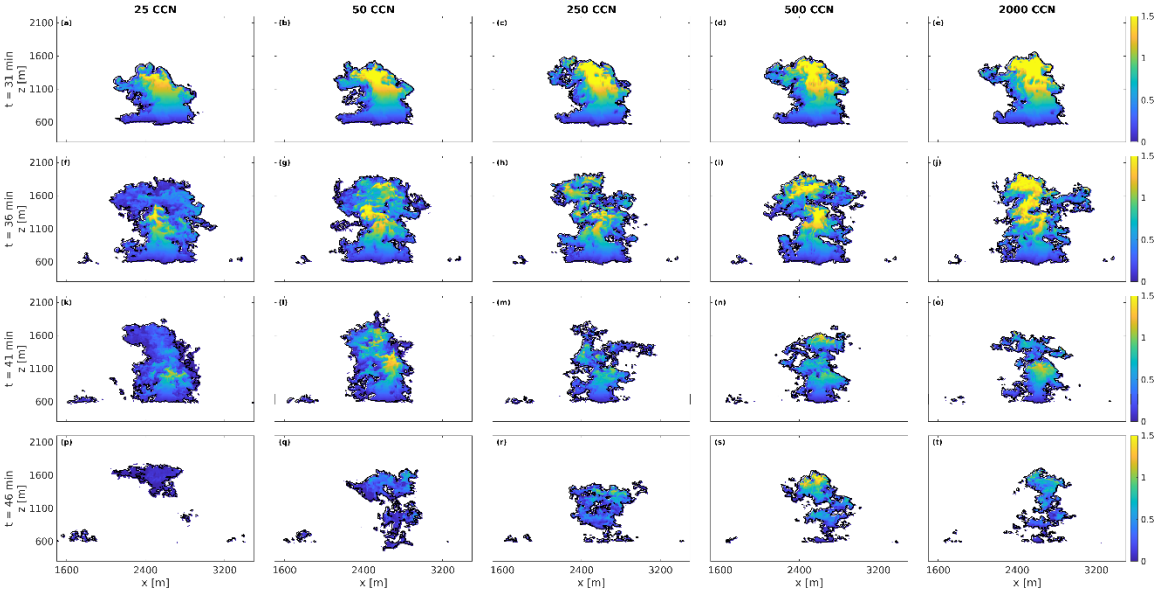


Figure S2: Same as Figure 1, but showing only cloud-droplet liquid water content (bins 1–15), excluding precipitation-sized drops.

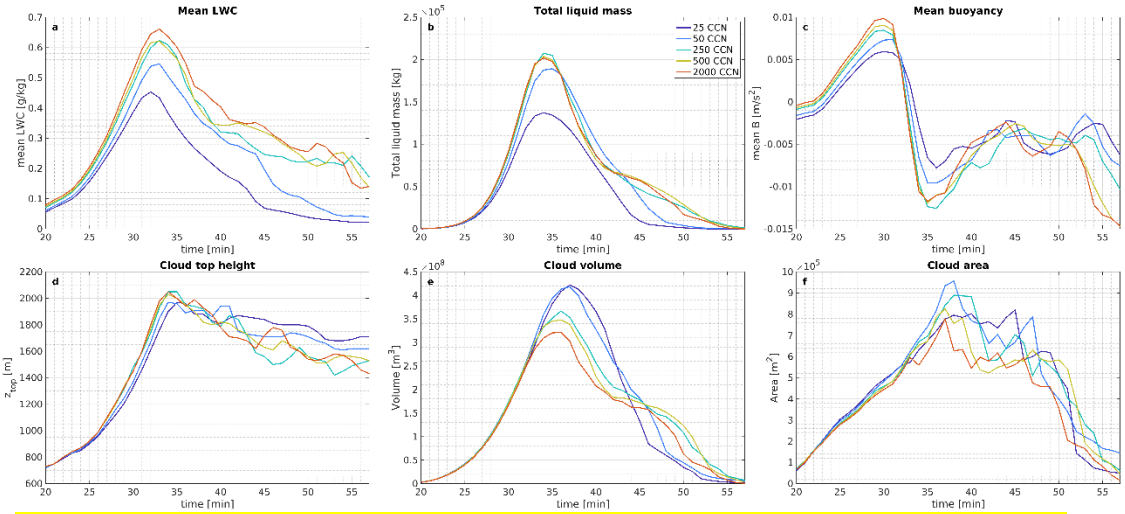


Figure S3: Same as Figure 2, but showing only cloud-droplet liquid water content (bins 1–15), excluding precipitation-sized drops.

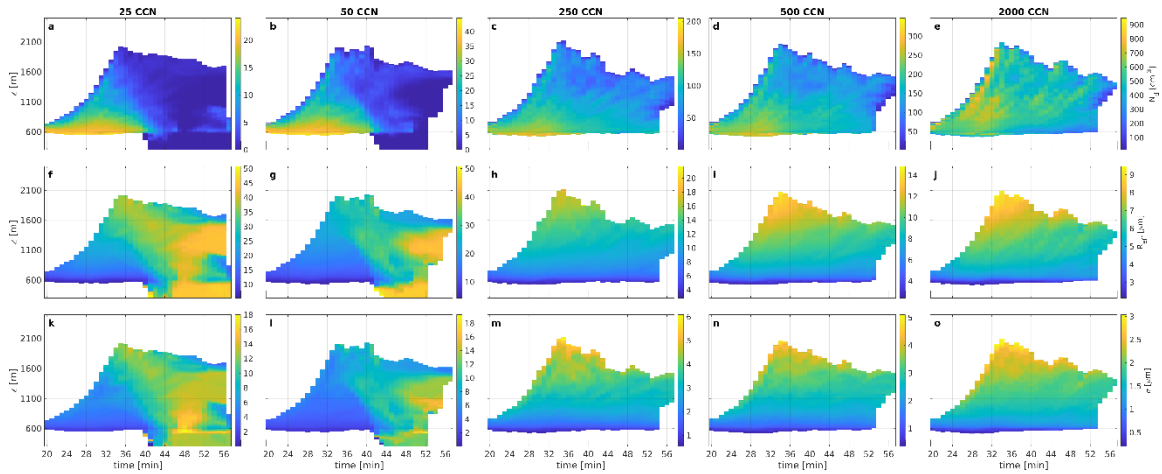


Figure S6: Same as Figure S5, but showing only cloud-droplet liquid water content (bins 1–15), excluding precipitation-sized drops.

3) Section 2 requires additional detail for reproducibility.

This concern can be addressed relatively easily. At present, the model description is too brief for an independent investigator to readily reproduce the simulations.

Beyond the description of the HUCM spectral-bin framework, the SAM configuration should be documented more completely. For example:

- How is the model top boundary treated? Is a damping or sponge layer employed?
- Which radiation scheme is used?
- How is subgrid-scale turbulence parameterized?
- Is the sub-cloud CCN concentration replenished continuously or only initialized at t = 0?
- How does the aerosol regeneration scheme operate in practice, and under what conditions does it affect the simulation?

Finally, while the BOMEX setup is standard within the shallow-convection community, it may not be familiar to all ACP readers. A brief summary of the thermodynamic initialization and forcing in either the manuscript or supplementary material would improve accessibility.

Answer: We thank the reviewer for this helpful comment. We have expanded Section 2 to provide a more complete description of the SAM configuration and simulation setup and thereby improve the reproducibility of the simulations.

These additions have been incorporated into the revised Section 2:

"We used the System for Atmospheric Modeling (SAM) (Khairoutdinov and Randall, 2003) coupled with the Spectral Bin Microphysics (SBM) scheme (Khain et al., 2004) and an aerosol regeneration scheme (Arieli et al., 2025b, a) to simulate trade cumulus clouds following the Barbados Oceanographic and Meteorological Experiment (BOMEX) case setup (Siebesma et al., 2003; Friedman et al., 1970). The setup includes large-scale forcing and is initialized with vertical profiles of

water vapor mixing ratio and potential temperature, with an inversion layer located between approximately 1500 and 2000 m. These profiles represent a trade-wind boundary layer consisting of a near-surface mixed layer, an overlying cloud layer, and a strong inversion. The surface fluxes were kept constant, and the background advection was set to zero to maintain the cloud near the center of the domain. Cloud initiation was triggered using a thermal perturbation of 0.1 K. The perturbation's radius was 500 m, with a depth of 100 m extending upward from the surface. Its magnitude decreased from the center toward the edge following a cosine-squared function, and random noise was superimposed on the perturbation to initiate turbulent motions. Subgrid-scale turbulence was parameterized using a prognostic 1.5-order turbulent kinetic energy (TKE) closure scheme. Interactive radiative transfer was not included in the simulations. Instead, radiative cooling was prescribed through the BOMEX large-scale forcing, with a cooling rate of approximately 2 K day $^{-1}$ below 1500 m, gradually decreasing in magnitude with height between 1500 and 2500 m, and reaching zero at 2500 m.

In the SBM scheme, dry aerosol particles are represented using 39 size bins with radii up to 8 μm, and cloud droplets are represented using 33 size bins starting at 2 μm. Activation is explicitly treated according to Köhler theory: at each time step, the critical dry aerosol radius is diagnosed from the local supersaturation, and dry aerosol bins with radii larger than this critical value are activated into droplets, after which the corresponding dry aerosol bins are emptied. Dry aerosols smaller than 0.33 μm are transferred to the smallest droplet bin (2 μm), whereas droplets formed on larger aerosols are assigned to droplet bins corresponding to a radius equal to six times the dry aerosol radius, following Kogan (1991).

Aerosol particles are regenerated following complete droplet evaporation. When a droplet evaporates to a radius smaller than 2 μm, the aerosol contained within it is returned to the surrounding dry-aerosol size distribution according to its mass. The mean dry-aerosol size is estimated from the total aerosol mass and droplet number concentration within each size bin, and a remapping procedure is applied when the resulting aerosol size does not coincide with the bin size in the dry-aerosol grid. For every drop that completely evaporates, one regenerated aerosol particle is released back to the atmosphere. These regenerated aerosol particles can subsequently reactivate and form additional cloud droplets if they encounter the required supersaturated conditions (Arieli et al., 2025b, a).

We performed five single-cloud simulations with initial aerosol number concentrations of 25, 50, 250, 500, and 2000 cm^{-3}, uniformly distributed below cloud base, from the surface up to 600 m. The aerosol population was prescribed only at the beginning of the simulation, with no subsequent external addition of CCN. The model domain was 5.12 km × 5.12 km in the horizontal with cyclic boundary conditions. Gravity-wave damping was applied at the top of the domain, while the temperature and water-vapor gradients were maintained. The horizontal grid spacing was dx = dy = 10 m. The vertical grid spacing was dz = 10 m up to 3 km and 50 m in the uppermost kilometer, well above the cloud-top height. The model time step was dt = 0.5 s."

Minor comments

- Title: Consider replacing "Shallow Cumulus" with "Shallow Trade Cumulus". Important dynamical differences exist between trade cumulus and shallow continental or higher-latitude cumulus clouds.

  Answer: We thank the reviewer for this suggestion. We have revised the title by replacing "Shallow Cumulus" with "Shallow Trade Cumulus" to more accurately reflect the atmospheric conditions examined in this study. We have also updated the terminology in other relevant sections of the manuscript to maintain consistency.

- Line 81: Please comment on the potential role of modern scanning radar and lidar observations for studying the lifecycle of shallow cumulus clouds.

  Answer: Thank you for this important suggestion. We have revised the Introduction to acknowledge the potential role of modern ground-based radar and lidar observations in studying the lifecycle of shallow cumulus clouds, while also noting their observational limitations. The revised text reads:

  "Satellite observations often provide instantaneous snapshots of cloud fields, which limits the ability to diagnose life cycle-dependent behavior and related feedback (Quaas et al. 2020). Geostationary platforms can partially address this limitation by offering time-resolved observations over a fixed region, but typically at the cost of reduced spatial and spectral detail compared with polar-orbiting sensors. Modern scanning cloud radars can track individual shallow cumuli along their lifecycle, from formation to dissipation; however, maintaining continuous observations of the same cloud can be challenging because of the narrow radar beam, and the cloud motion, which can move the cloud out of the sampled region. In addition, the measurements often represent only a two-dimensional slice rather than the full three-dimensional cloud structure (Borque et al., 2014). Lidar provides complementary high-resolution information on cloud boundaries and droplet structure, but its signal can weaken significantly or even become completely attenuated within the cloud, limiting its capability to represent the full cloud depth (Kalesse-Los et al., 2022; Yeom et al., 2026). As a result, directly constraining the full evolution of individual shallow cumuli remains observationally challenging."

- Figure 2 (and other time series): The yellow curve used for CCN2000 is difficult to see. Consider a darker colour.

  Answer: We thank the reviewer for this suggestion. We have changed the color used for CCN2000 to a darker color in Figure 2 and Figure 4 to improve its visibility.

- Cloud splitting is briefly mentioned in the Methods section but not discussed further. How much liquid water mass is lost through splitting during the simulations? Does the importance of splitting increase during dissipation or at higher CCN concentrations?

  Answer: We thank the reviewer for this comment. To quantify the influence of cloud splitting on the tracking analysis, we calculated the liquid water mass contained in fragments that split from the tracked main cloud and were excluded by the tracking algorithm at each time step, as well as its fraction relative to the total liquid water mass of all descendant fragments. Only fragments originating from the initially triggered main cloud were included in

this calculation. Secondary clouds which formed independently were excluded from the analysis and did not contribute to the reported splitting mass.

We have added a description of this analysis and a brief discussion of the results to the Methods section, with the corresponding results presented in the Supplementary Information (Fig. S1).

The results show that the excluded liquid water mass is generally small during the early stages of cloud evolution, while larger, intermittent splitting events occur during the later stages, particularly during dissipation. The excluded mass also tends to increase with CCN concentration, although this relationship is not strictly monotonic. The maximum excluded mass ranges from approximately 600 kg in the 50 CCN case to 4,133 kg in the 2000 CCN case. In the latter, this corresponds to approximately 19.5% of the total descendant liquid water mass.

These findings indicate that splitting has a relatively limited influence on the tracked cloud during the early stages but can become more important during dissipation, particularly in the more polluted simulations.

The revised method:

"A cloud identification procedure was used to isolate the main cloud generated by the initial thermal perturbation, excluding secondary clouds from the analysis. In the spectral-bin microphysics scheme, cloud droplets are represented by bins 1-15, with bin 15 corresponding to a droplet radius of 50.8 μm, whereas bins 16-33 represent raindrops. Cloud objects were identified using the total liquid water mixing ratio, defined as the sum of cloud-droplet water and rainwater (all 33 bins), with a threshold of $LWC = 0.01 \frac{g}{kg}$*. The main cloud was initially identified as the largest connected cloud object and subsequently tracked based on its spatial overlap with the cloud identified at the previous time step. When the tracked cloud split into multiple connected objects, only the largest fragment was retained as the continuation of the main cloud, while the remaining fragments were excluded from the subsequent cloud analysis. These excluded fragments were distinguished from unrelated secondary clouds by their spatial overlap with the previously tracked cloud. To evaluate the influence of splitting on the analysis, we calculated the total liquid water mass of the excluded fragments at each time step. This mass was also expressed as a fraction of the combined liquid water mass of the retained main cloud and all fragments identified as splitting from it at that time step (Fig. S1). The results show that the liquid water mass associated with the excluded fragments is generally small during the early stages of cloud evolution, whereas larger, intermittent splitting events occur during the later stages."*

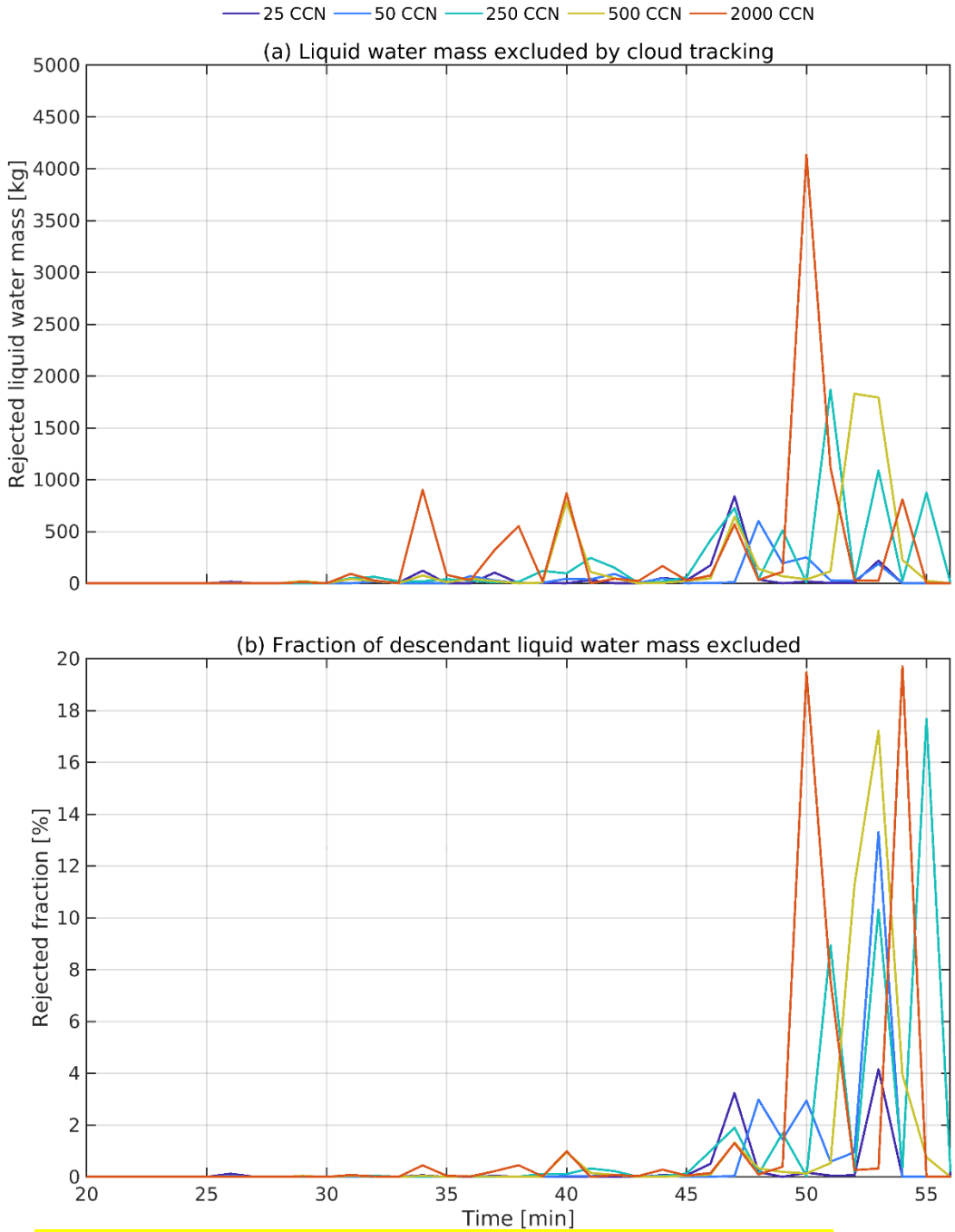


Figure S1: Influence of cloud splitting on the tracking analysis for the five CCN concentrations. (a) Instantaneous liquid water mass contained in secondary cloud fragments excluded by the tracking algorithm. (b) Corresponding rejected mass expressed as a percentage of the total liquid water mass of all linked descendant fragments. Only the dominant fragment is retained in the analysis.

- Figure 3b: Please comment on the apparent loss of cloud/sub-cloud values near 52 minutes in the CCN50 simulation.

Answer: We thank the reviewer for this comment. The Hovemollers in figure 3 are tracking the cloud according to LWC that contains both droplets and raindrops. Precipitation below cloud base can therefore be included in the analysis as long as it remains connected to the tracked main cloud. However, around 52–53 min in the CCN50 simulation, the descending precipitation region becomes disconnected from the upper cloud. The tracking algorithm continues to follow the upper cloud, while the detached precipitation region is excluded from the analysis. This explains the apparent disappearance of the lower-level and subcloud values in Figure 3, even though precipitation may still be present in the simulation. At other times, precipitation below cloud base remains visible because it is still included in the tracked cloud object. We have clarified this behavior in the revised manuscript section 3.1.2:

"In the 50 CCN simulation, the apparent disappearance of lower-level and subcloud values around 52-53 min (Fig. 3b,g) is related to the cloud-tracking procedure. At this time, the descending precipitation becomes disconnected from the main cloud, and the tracking algorithm continues to follow only the upper cloud, excluding the detached precipitation from the analysis (see Fig. S4) . Thus, the disappearance of these values reflects the tracking procedure rather than a sudden disappearance of precipitation from the simulation."

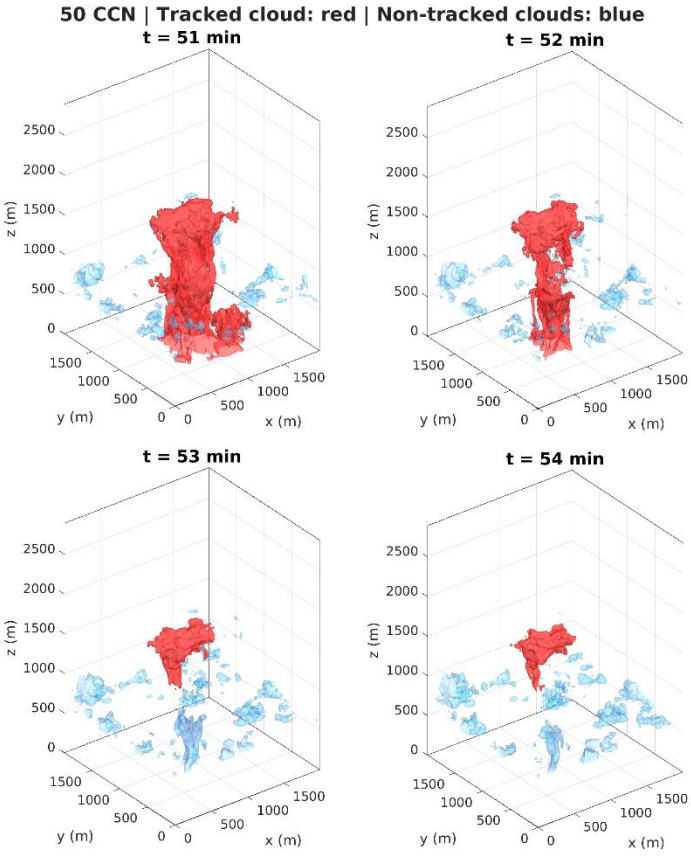


Fig S4: Three-dimensional visualization of the tracked cloud in the 50 CCN simulation at 51, 52, 53, and 54 min. Red surfaces represent the tracked cloud, while blue surfaces represent other, non-tracked clouds. Clouds are identified using a total liquid water mixing ratio threshold of 0.01 $\frac{g}{kg}$.

- Figure 3: For the precipitating simulations (CCN25 and CCN50), why is there relatively little evaporation below cloud base? What is the mean relative humidity below 600 m?

  Answer: We thank the reviewer for this comment. The relatively weak evaporation below cloud base in the precipitating simulations (CCN25 and CCN50) can be explained by the relatively humid subcloud environment. The mean relative humidity below 600 m increases from approximately 80% at 100 m to 93% at 550 m. These relatively moist conditions, particularly near cloud base, reduce the vapor pressure deficit and therefore limit evaporation, helping to explain the relatively weak evaporation tendency observed below cloud base in Figure 3.

  The revise section 3.1.2:

  "In the precipitating clouds, evaporation extends rapidly downward as precipitation-induced downdrafts develop. These downdrafts enhance downward transport and mixing, while the evaporation of falling hydrometeors promotes evaporative cooling and further strengthens the descending motion. As a result, evaporation affects a larger fraction of the cloud depth. However, evaporation below cloud base remains relatively weak, which may be partly explained by the humid subcloud environment. The mean relative humidity increases from approximately 80% at 100 m to 93% at 550 m, indicating relatively moist conditions that limit the evaporation of falling raindrops."

- Line 190: "...vertical velocity within the cloud..."

  Answer: Thank you. The revised text: *"Figure 3a–e shows a Hovmöller diagram of the horizontally averaged vertical velocity within the cloud at each height level as a function of time"*

- Line 248: Define DSD width explicitly as the standard deviation of the size distribution.

  Answer: Thank you, the revised text: *"Figure 5f–o shows two additional parameters, effective radius (Fig. 5f-i) and DSD width (standard deviation; Fig. 5k-o), for a full description of the evolution of the droplet size distribution (DSD)."*

- Line 254: Please define "secondary nucleation". This term has a specific meaning in ice-phase cloud physics and may be confusing in the present context.

  Answer: Thank you. The revised text: *"The DSD standard deviation (Fig. 5m-o) also tends to increase with height, but with a noisier and less smooth pattern, reflecting enhanced mixing near cloud top together with collision–coalescence and new droplet formation."*

- Lines 255-257: This discussion is difficult to follow. If turbulent mixing acts more slowly, how does that reconcile with the subsequent statement regarding droplets being exposed to entrained dry air? Please clarify the physical interpretation.

  Answer: Thank you. The revised text: *"This behavior further suggests that the microphysical response to mixing occurs on a shorter timescale than the mixing process itself. As dry environmental air is progressively entrained into the cloud, droplets exposed to this air can evaporate rapidly, leading to a reduction in droplet number concentration while maintaining a relatively similar mean droplet radius."*

- Line 256: "...than the microphysical response..." Response to what? Entraining dry air? Turbulent mixing? Thermodynamic perturbations?

  Answer: Thank you. The revised text: *"This behavior further suggests that the microphysical response to mixing occurs on a shorter timescale than the mixing process itself. As dry environmental air is progressively entrained into the cloud, droplets exposed to this air can evaporate rapidly, leading to a reduction in droplet number concentration while maintaining a relatively similar mean droplet radius."*

- Line 259: This discussion seems more appropriate for the Conclusions section.

  Answer: Thank you. This paragraph moved to the conclusion section.

- Figure 6: Please comment explicitly on the non-linear variation in the colour-bar ranges across CCN concentrations.

  Answer: We thank the reviewer for this comment. The color-bar ranges in Figure 6 were adjusted individually for each simulation to better visualize the spatial and temporal evolution of the nucleation and collision tendencies, which differ substantially in magnitude across the different simulations (with various CCN concentrations). The maximum nucleation tendencies do not exhibit a monotonic dependence on CCN concentration, whereas the collision tendencies decrease strongly with increasing CCN concentration, In particular, collision tendencies are substantially larger in the low-CCN precipitating cases than in the high-CCN non-precipitating cases, reflecting the stronger collision–coalescence processes associated with precipitation formation. As a result, the color-bar ranges vary nonlinearly across the simulations. We have clarified the use of different color scales and their interpretation in the revised section 3.2.2.

  "The collision–coalescence tendency evolves differently. Its magnitude decreases strongly with increasing CCN concentration, with substantially higher values in the precipitating cases than in the non-precipitating cases. It peaks near the time of maximal cloud growth, when the liquid water content and updraft strength are the largest (see Fig. 1), and then decreases as the cloud dissipates. In the precipitating clouds, the region of enhanced collision–coalescence extends downward following the onset of precipitation, reflecting the formation and descent of rain."

- Line 282: Please clarify how DFCE is defined. Is it calculated from the nearest cloud edge at the same height, or the minimum distance to any cloud boundary in three-dimensional space? This becomes particularly important for the values reported above cloud top.

  Answer: We thank the reviewer for pointing out that the definition of DFCE was not sufficiently clear. DFCE is calculated as the horizontal distance from the nearest cloud edge at the same height level. The calculation is performed independently at each height level, and if no cloud is present at a given height, DFCE is not defined at that height. We have clarified this definition in the revised manuscript.

  "Here, DFCE is defined only within the cloud interior as the horizontal distance from the cloud edge at the same height level. Negative values correspond to increasing distance from the cloud edge toward the cloud center."

"Figure 11a-e presents Hovmöller diagrams of E as a function of distance from the cloud edge, with DFCE defined here only outside the cloud, as the horizontal distance from the cloud edge at the same height level. Larger values correspond to locations farther into the surrounding environment."

- Figure 12: Consider using a consistent colour scale across all panels.

  Answer: We thank the reviewer for this suggestion. We have revised Figure 12 to use a consistent color scale across all panels, allowing for a more direct comparison between the simulations.

Typographical corrections

- Line 53: "cumulus" (not Cumulus)
- Line 89: "simple"
- Line 93: "accurately"
- Line 155: "life cycle"
- Line 340: "life cycle"

Answer: We thank the reviewer for pointing out these typographical errors. All of them have been corrected in the revised manuscript.

Reviewer #2:

This manuscript investigates the dissipation stage of isolated shallow cumulus clouds using high-resolution SAM–SBM simulations under BOMEX conditions, spanning five CCN concentrations (25–2000 cm^{-3}). The key findings are that dissipation is a prolonged, oscillatory, spatially non-uniform stage; that its dynamics and microphysics differ fundamentally depending on aerosol loading and precipitation; and that dissipating clouds leave detectable vorticity and humidity signatures in their surroundings. The manuscript addresses an important and relatively underexplored topic, and aims to improve process-level understanding for convection parameterization and the interpretation of satellite snapshot observations. However, several issues require revisions to address as I mentioned below:

1. All simulations track a single, thermally triggered cloud. The authors briefly acknowledge this limitation in the Conclusions but do not quantify how the results depend on domain size, cloud size, or the absence of cloud–cloud interactions. Given that the paper's stated motivation includes improving parameterizations and interpreting satellite snapshots of cloud fields, a discussion on how multi-cloud interactions might modify the dissipation signatures is warranted.

   Answer: Thank you for this important comment. We agree that the use of a single, thermally triggered cloud limits the extent to which our results can be generalized to naturally evolving cloud fields. The present simulations were intentionally designed to isolate the dissipation of an individual cloud. Although the sensitivity to domain size and cloud size could be investigated using additional single-cloud simulations, these parameters were not systematically varied in the present study, and their influence therefore cannot be

quantified. Nevertheless, the horizontal model domain (5.12 km × 5.12 km) is considerably larger than the simulated cloud, which is expected to limit the influence of the lateral boundaries on its evolution. Assessing cloud–cloud interactions requires simulations of multiple interacting clouds and is beyond the scope of the present study. We have therefore expanded the Conclusions to discuss, based on previous studies, how cloud–cloud interactions may modify the timing and duration of dissipation and its associated turbulence and humidity signatures. We also clarify that the present findings characterize isolated shallow trade cumulus clouds under the investigated BOMEX conditions and that extending the analysis to interacting cloud populations is an important direction for future work.

We have added the following paragraph to the Conclusions:

"*A limitation of this study is that the simulations consider a single, thermally triggered cloud, excluding cloud–cloud interactions and their potential influence on the dissipation stage. Previous studies have shown that interactions between neighboring clouds can affect cloud evolution through merging, splitting, compensating downdrafts, and changes in environmental moisture (Chen et al., 2023), as well as modifying cloud development and slowing dissipation through enhanced updrafts and moisture supply (Xu et al., 2026). Such interactions may influence the timing and duration of dissipation and complicate the identification of its associated turbulence and humidity signatures within cloud fields. Therefore, the findings presented here characterize the dissipation of isolated shallow trade cumulus clouds under the investigated BOMEX conditions. Future studies of interacting cloud populations are therefore needed to assess how these findings extend to cloud fields.*"

2. BOMEX includes background wind shear, yet the authors set background advection to zero. The omission of shear is potentially significant: shear can strongly affect cloud tilt, entrainment and detrainment patterns, and the spatial distribution of the humid halo. The authors should explicitly justify this choice and discuss how the results might differ under realistic shear.

Answer: We thank the reviewer for this comment that helped us clarify our method. This work presents a case study of isolated shallow warm clouds developing within a marine boundary layer. In the present case, the wind shear within the cloud-bearing boundary layer is relatively weak. We therefore chose to omit the background advection, allowing the simulated cloud to remain near the center of the computational domain and thereby facilitating the tracking and detailed analysis of the cloud throughout its life cycle at very high spatial and temporal resolution. This choice also allowed us to focus on the processes associated with cloud dissipation while limiting additional dynamical complexity.

We agree, however, that stronger environmental wind shear could influence cloud geometry and tilt, entrainment and detrainment, and consequently the spatial distribution of the humid and turbulent signatures surrounding the cloud. Therefore, the quantitative spatial patterns reported here may differ under conditions with stronger shear. Investigating these effects would require extending the present analysis to simulations that explicitly vary the environmental wind profile and is an important direction for future work, particularly at the cloud-field scale. We added a discussion of this limitation in the revised manuscript.

The revised conclusions: *"This study focuses on the BOMEX case study, which represents an idealized shallow trade cumulus environment. BOMEX is a well-studied and widely validated benchmark for shallow convection. We therefore expect many of the processes identified here to be representative of trade cumulus clouds. Moreover, several features of the simulated dissipation stage are consistent with previous in situ observations and numerical studies, providing additional support for the robustness of our results. Nevertheless, the extent to which these findings can be generalized beyond the present conditions remains uncertain. Environmental conditions such as stronger wind shear, deeper or shallower convection, or different atmospheric stability may alter the structure and evolution of cloud dissipation. For example, stronger shear may affect cloud tilt, entrainment and detrainment, and the spatial distribution of the surrounding humid and turbulent signatures."*

3. The manuscript does not mention whether radiative transfer is included in the simulations. Radiative cooling at cloud top can significantly influence dissipation rates and the development of the near-cloud environment (e.g., humidity halos). The authors should clarify the radiation configuration and discuss its potential impact.

   Answer: Thank you for this important comment. We have clarified the radiation configuration in the Methods. Interactive radiative transfer was not included in the simulations; however, radiative cooling was represented through the prescribed large-scale forcing following the BOMEX configuration (Siebesma et al., 2003). The prescribed cooling rate is approximately 2 K day^{-1} below 1500 m and decreases to zero at 2500 m.

   We agree that the absence of cloud-dependent radiative effects represents a limitation of the present study. Previous studies have shown that interactive radiation can influence shallow cumulus dynamics and cloud evolution (Jiang and Cotton, 2000; Klinger et al., 2017). In particular, cloud-top radiative cooling may modify buoyancy, turbulent mixing, and entrainment, potentially affecting the timing and duration of dissipation and the evolution of the near-cloud humidity and turbulence signatures. Since our simulations do not explicitly resolve these cloud-dependent radiative effects, their influence cannot be quantified from the present results. At the cloud-field scale, radiative effects also depend on cloud fraction and the spatial organization of clouds. Since our simulations focus on a single, isolated cloud, they were not designed to investigate these cloud-field-scale radiative feedbacks. We therefore consider the role of interactive radiation an important topic for future simulations of shallow cumulus cloud fields, where cloud fraction and cloud–cloud interactions can be represented. We have clarified this limitation and the direction for future research in the Conclusions.

   The revised conclusions: *"This study focuses on the BOMEX case study, which represents an idealized shallow trade cumulus environment. BOMEX is a well-studied and widely validated benchmark for shallow convection. We therefore expect many of the processes identified here to be representative of shallow trade cumulus clouds. Moreover, several features of the simulated dissipation stage are consistent with previous in situ observations and numerical studies, providing additional support for the robustness of our results. Nevertheless, the extent to which these findings can be generalized beyond the present conditions remains*

uncertain. Environmental conditions such as stronger wind shear, deeper or shallower convection, or different atmospheric stability may alter the structure and evolution of cloud dissipation. In particular, stronger shear may affect cloud tilt, entrainment and detrainment, and the spatial distribution of the surrounding humid and turbulent signatures. In addition, cloud-dependent radiative effects were not represented in the simulations. These effects may influence cloud-top dynamics and mixing, potentially modifying the dissipation process and the associated turbulence and humidity signatures. Because radiative feedbacks at the cloud-field scale also depend on cloud fraction and the spatial organization of clouds, their influence on dissipation should be investigated in future simulations of shallow cumulus cloud fields that include interactive radiation."

The revised methods:

"Interactive radiative transfer was not included in the simulations. Instead, radiative cooling was prescribed through the BOMEX large-scale forcing, with a cooling rate of approximately 2 K day^{-1} below 1500 m, decreasing to zero at 2500 m."

4. The authors define dissipation onset as the time when cloud-mean buoyancy turns negative and cloud-top height ceases to rise. However, the paper itself demonstrates that lower cloud layers can remain positively buoyant with active pulse-like updrafts long after upper-level decay begins, meaning different vertical layers occupy different lifecycle stages simultaneously. The work does not quantitatively compare this definition to established alternative frameworks (e.g., the normalized total-water "cloud clock" of Witte et al., 2014; the percentile-based buoyancy/velocity classification of Katzwinkel et al., 2014) or assess how sensitive reported dissipation durations and characteristics are to the chosen threshold. How to demonstrate the advantages of the concept of dissipation as defined in this article?

   Answer: We thank the reviewer for raising this point. Indeed no single bulk definition can fully represent the life-cycle stage of all parts of a trade cumulus cloud, particularly when multiple pulses occur and different vertical levels evolve asynchronously. Our definition is therefore not intended to imply that the entire cloud enters dissipation simultaneously, but rather to provide a consistent and physically motivated reference time for the transition from overall cloud development to decay in a continuously tracked cloud.

   Alternative classifications have related limitations. In particular, Witte et al. (2014) showed that their normalized-total-water "cloud clock" is most effective for single-pulse clouds, whereas additional buoyant pulses can complicate the assignment of a unique cloud age because growth and dissipation may occur simultaneously in different parts of the cloud. The classification of Katzwinkel et al. (2014), based on the 90th percentiles of vertical velocity and buoyancy, provides a useful framework for classifying instantaneous cloud observations, whereas our analysis follows the same cloud continuously throughout its lifetime. The main advantage of our approach in the context of this study is that it combines the temporal evolution of cloud-mean buoyancy and cloud-top height to identify the transition from overall cloud growth to decay, even when lower cloud levels remain positively buoyant and upward motion persists. These two variables also provide a useful basis for defining the life-cycle stages because their temporal evolution is relatively consistent across the different CCN cases, despite differences in precipitation development. To assess the

consistency between these two indicators, we compared the time at which cloud-mean buoyancy first becomes negative with the time at which cloud-top height reaches its maximum. Across all five simulations, the difference between these two times does not exceed 3 minutes. This indicates that both indicators identify a similar transition period, although they do not necessarily coincide. Furthermore, using either indicator individually would shift the estimated dissipation onset by no more than 3 minutes, providing a quantitative estimate of the sensitivity of the onset time to the choice between these two criteria. Their combined use therefore provides a consistent reference point for comparing the subsequent evolution of cloud dynamics, turbulence, microphysics, and the surrounding environment across the different CCN simulations.

Importantly, the evolution from growth to advanced dissipation is also reflected in changes in cloud dynamics, turbulence, and the near-cloud environment, although these properties do not necessarily change at the same time. Our definition therefore identifies a reference time for the transition in the overall evolution of the tracked cloud, rather than implying that dissipation begins simultaneously at all heights. Our vertically resolved analysis demonstrates that lower cloud levels may remain positively buoyant and dynamically active even after cloud-mean buoyancy has become negative and cloud-top height has stopped increasing. Thus, our classification describes the overall cloud evolution while recognizing that different vertical levels may occupy different dynamical stages simultaneously. We have revised the manuscript to clarify both the rationale and the limitations of our definition and to emphasize that the defined dissipation onset represents a bulk-cloud reference time rather than a simultaneous transition at all heights. The revised results:

"*The dissipation stage begins around 33–35 min, when the cloud-mean buoyancy becomes negative, and the cloud's top stops rising. Across all five simulations, the time difference between the first occurrence of negative cloud-mean buoyancy and the maximum cloud-top height does not exceed 3 minutes, indicating that the two indicators identify a relatively similar transition period and supporting their combined use in defining the onset of dissipation. Within this definition, the dissipation stage lasts longer than the growth and mature stages combined. During this stage, the cloud no longer exhibits sustained vertical growth: cloud-top height decreases on average, although it continues to oscillate. At the same time, the mean buoyancy becomes negative overall, but also oscillates and can temporarily return to positive values. These oscillations are consistent with the cloud interacting with the very stable inversion layer, where oscillatory motions can be expected. Thus, the onset of negative mean buoyancy together with a decrease in cloud-top height and the subsequent oscillatory behavior of both variables provides a more robust indication of dissipation than buoyancy alone. Importantly, this classification represents the overall cloud evolution rather than a simultaneous transition throughout the cloud. As shown by the vertically resolved analysis below, lower cloud levels can remain positively buoyant and dynamically active even after the bulk-cloud dissipation stage has begun. The dynamical progression underlying this stage classification is qualitatively consistent with that described by Katzwinkel et al. 2014, who classified cloud stages based on the 90th percentiles of in-cloud buoyancy and vertical velocity measured along individual cloud transects. In their framework, negatively buoyant clouds with persistent updrafts are classified as decelerated, whereas negatively buoyant clouds with downdrafts are classified as dissipating. Our*

definition, however, identifies the onset of bulk-cloud dissipation while upward motion may still persist in parts of the cloud, reflecting the vertically nonuniform nature of this transition."

5. Line 89: "simpale" → "simple." Answer: It was corrected, thank you.
6. Line 92: "accuratly" → "accurately." Answer: It was corrected, thank you.
7. Line 102: "reported bySchmeissner" — missing space before "Schmeissner." Answer: It was corrected, thank you.
8. Figure 2 caption: Panels (d), (e), and (f) are all labeled "(d)." Please correct to (d), (e), (f). Answer: It was corrected, thank you.
9. Figure 9 caption: States "Results are shown for the simulation initialized with 500 cm^{-3} CCN," but the text (Section 3.2.3) clearly indicates this figure corresponds to the 50 cm^{-3} (precipitating) case.

   Answer: It was corrected, thank you.